

ORIGINAL ARTICLE

WILEY

How muscles maximize performance in accelerated sprinting

Marcus G. Pandy¹ | Adrian K. M. Lai² | Anthony G. Schache^{1,3} | Yi-Chung Lin¹

¹Department of Mechanical Engineering, University of Melbourne, Parkville, Victoria, Australia

²Department of Biomedical Physiology and Kinesiology, Simon Fraser University, Burnaby, Canada

³La Trobe Sport and Exercise Medicine Research Centre, La Trobe University, Bundoora, Australia

Correspondence

Marcus G. Pandy, Department of Mechanical Engineering, University of Melbourne, Parkville, Victoria 3010, Australia.

Email: pandym@unimelb.edu.au

Funding information

Australian Research Council, Grant/Award Number: LP110100262

We sought to provide a more comprehensive understanding of how the individual leg muscles act synergistically to generate a ground force impulse and maximize the change in forward momentum of the body during accelerated sprinting. We combined musculoskeletal modelling with gait data to simulate the majority of the acceleration phase (19 foot contacts) of a maximal sprint over ground. Individual muscle contributions to the ground force impulse were found by evaluating each muscle's contribution to the vertical and fore-aft components of the ground force (termed “supporter” and “accelerator/brake,” respectively). The ankle plantarflexors played a major role in achieving maximal-effort accelerated sprinting. Soleus acted primarily as a supporter by generating a large fraction of the upward impulse at each step whereas gastrocnemius contributed appreciably to the propulsive and upward impulses and functioned as both accelerator and supporter. The primary role of the vasti was to deliver an upward impulse to the body (supporter), but these muscles also acted as a brake by retarding forward momentum. The hamstrings and gluteus medius functioned primarily as accelerators. Gluteus maximus was neither an accelerator nor supporter as it functioned mainly to decelerate the swinging leg in preparation for foot contact at the next step. Fundamental knowledge of lower-limb muscle function during maximum acceleration sprinting is of interest to coaches endeavoring to optimize sprint performance in elite athletes as well as sports medicine clinicians aiming to improve injury prevention and rehabilitation practices.

KEYWORDS

gluteal, hamstring, impulse, plantarflexor, propulsion, running

1 | INTRODUCTION

The best sprinters run at an average speed of approximately 10 m/s and can reach maximum speeds of nearly 13 m/s during a 100 m race.¹ This level of exceptional performance is achieved by maximally accelerating the body during the first half of the race and maintaining that momentum thereafter. The force generated on the ground at each foot contact creates an impulse that causes the necessary increase in forward momentum of the body's center of mass. The lower-limb muscles together with the actions of gravity and inertia

generate the required ground force impulse, but the overall contribution from the muscles is by far the greatest.^{2,3}

Many investigators have performed inverse dynamics analyses to determine the net moments exerted by the lower-limb joints for sprinting at a steady-state speed.⁴⁻⁶ Recent studies also have estimated the forces developed by the leg muscles for running at various steady-state speeds, including sprinting.^{2,3,7} Soleus, gastrocnemius and vasti were found to be the major contributors to the vertical (support) and fore-aft (propulsive/braking) components of the ground reaction force (GRF) at all steady-state running speeds.^{2,3}

Fewer biomechanical analyses of the acceleration phase of sprinting have been published, due largely to the challenges associated with recording body-segmental motion and GRFs for multiple steps of high-speed running. Indeed, only one or two representative steps are typically analyzed in studies of accelerated sprinting.⁸⁻¹⁰ Rabita et al.¹¹ measured step length, step frequency, and all three components of the GRF from seven separate sprint trials and reconstructed a single virtual 40-meter sprint (18 foot contacts). They found that step length increased linearly with running speed while step frequency remained relatively constant after block clearance. This result indicates that stance phase mechanics dominates performance in accelerated sprinting because increases in step length, and hence running speed, are due primarily to higher ground force impulses generated during stance. Nagahara et al.¹² measured the GRF for all 28 foot contacts of a single 60-m sprint and found that performance was dependent not only on the exertion of large propulsive forces throughout the acceleration phase but also on the suppression of braking forces as runners approached their maximum speed. Schache et al.¹³ computed the net moments exerted about the hip, knee and ankle joints for the majority of the acceleration phase of sprinting. They found that forward acceleration was linearly related to the impulses delivered by the hip-extensor and ankle-plantarflexor moments, and that the hip and ankle joints contributed a substantial fraction of the total positive work generated at each foot contact.

Less is known about the functional roles of the individual lower-limb muscles during maximum acceleration sprinting. To understand the function of the hamstrings, Morin et al.¹⁴ measured hip and knee joint torques using isokinetic dynamometry along with the fore-aft GRF and electromyographic (EMG) activity for select lower-limb muscles during short duration sprints on an instrumented motorized treadmill. A significant relationship was found between higher propulsive forces during sprinting and increased hamstring muscle activity during terminal swing as well as greater knee flexor eccentric peak torque, implying that the hamstring muscles are important for increasing speed during the first few steps of maximum acceleration sprinting.¹⁴ Other studies have drawn conclusions about the functional roles of individual muscles during sprinting based on muscle EMG recordings. For example, two such studies focused specifically on gluteus maximus and reported that this muscle acts to extend the hip and control trunk flexion during the stance phase of running and sprinting.^{15,16} A recent modelling study calculated lower-limb muscle forces for the first two foot contacts after block clearance and found that the ankle plantarflexors, soleus and gastrocnemius, contributed most of the GRF impulse generated at each step.¹⁷ There are no data that describe how individual muscles work synergistically to increase the forward momentum of the body beyond the first two foot contacts of accelerated sprinting. Fundamental knowledge of

muscle function during maximum acceleration sprinting is important for the design of athletic training regimens aimed at optimizing sprinting performance and for the development of more effective injury prevention and rehabilitation practices.

The overall goal of the present study was to provide a better understanding of how the lower-limb muscles maximize performance during accelerated sprinting. Our primary aim was to describe and explain the contributions of individual muscles to the vertical and fore-aft GRF impulses generated for the majority of the acceleration phase (19 foot contacts) of a maximal sprint. We were interested specifically in identifying those muscles responsible for increasing the forward momentum of the body at each step.

2 | METHODS

Five sub-elite sprinters (4 males, 1 female; age, 21.8 ± 3.2 years; height, 180.0 ± 8.3 cm; body mass, 73.6 ± 7.6 kg) with no pre-existing musculoskeletal injuries gave their informed consent to participate. All participants regularly competed in sprint events between 100 and 400 m, with personal best times for 100 m ranging from 10.4 s to 12.7 s. Approval was obtained from the relevant institutional ethics committees prior to commencement of the study.

Gait experiments were performed on a straight 110 m indoor track at the Biomechanics Laboratory of the Australian Institute of Sport in Canberra, Australia. Participants wore standard sprint-specific shoes consisting of a rigid carbon base-plate that allows minimal flexion at the metatarsophalangeal joint. Each participant was required to accelerate as quickly as possible from a static three-point crouched position (without starting blocks) until the end of the capture volume before decelerating to rest. Full-body motion, GRF, and muscle EMG data were recorded for the first 19 foot contacts of the acceleration phase in stages by adjusting the location of the starting position with respect to the first force plate. For example, to obtain data corresponding to the 19th foot contact, the starting position was shifted approximately 40 m away from the first force plate. A 3D motion analysis system with 22 VICON cameras (Oxford Metrics Ltd., Oxford, UK) each sampling at 250 Hz was used to measure full-body motion while GRFs were recorded from eight force plates (Kistler Instrument Corp., Amherst, NY, USA) each measuring 900×600 mm² in size and sampling at 1500 Hz. Muscle EMG data were recorded from five muscles: medial hamstrings (i.e., combined signals from semimembranosus and semitendinosus), vastus medialis and lateralis, lateral gastrocnemius, and soleus. Surface electrodes were placed on these muscles according to SENIAM recommendations.¹⁸ EMG signals were high-pass filtered using a 4th-order Butterworth filter with a cut-off frequency of 20 Hz, full-wave rectified,

and then low-pass filtered using a 4th-order Butterworth filter with cut-off frequency of 8 Hz. Full details of the experimental protocol are given by Lai et al.¹⁹

Computer simulations of the acceleration phase of sprinting were generated based on a generic model of the body.²⁰ The skeleton was represented as a 14-segment, 29-degree-of-freedom (dof) articulated linkage, with each hip modeled as a 3-dof ball-and-socket joint, and each knee and ankle represented as a 1-dof hinge joint. The torso articulated with the pelvis via a lumbar (back) joint. Each arm was represented by two segments, which were actuated by a 3-dof ball-and-socket shoulder joint and a 2-dof universal elbow joint. The lower-limb joints were actuated by 80 muscle-tendon units while the movements of the torso and arms were controlled by 13 ideal torque actuators. Each muscle-tendon unit was represented as a Hill-type muscle in series with tendon. The peak isometric force of each muscle was increased by a factor of two to more closely represent the overall leg strength of a sprinting athlete while each muscle's intrinsic maximum shortening velocity was assumed to be 20 optimal fiber lengths per second.² For all actuators other than the ankle plantarflexors, tendon strain was assumed to be 4.9% at the peak isometric force of the muscle.¹⁹ For the ankle plantarflexors, the strain in the Achilles tendon was assumed to be 10% at the peak isometric muscle force.¹⁹

Participant-specific musculoskeletal models were created by scaling the generic model to each participant's height and body mass. Participant-specific computer simulations of the first 19 foot contacts of the acceleration phase were then generated in OpenSim (v 3.3)²¹; altogether, 95 participant-specific simulations were generated for all 19 foot contacts across the 5 participants. An inverse kinematics analysis was performed to calculate the joint angular displacements by minimizing differences between the measured marker positions and the positions of corresponding virtual markers identified on the model. Next, the calculated joint kinematics along with the measured GRFs were filtered using a fourth-order, low-pass, Butterworth filter with a cut-off frequency of 15 Hz.¹⁹ The same cut-off frequency was used to filter both the motion and force data to avoid experimental impact artifacts in the calculation of the net joint moments.²² Finally, the filtered joint kinematics and GRFs were input to a Computed Muscle Control (CMC) algorithm²³ to generate a forward-dynamics simulation of each step of the acceleration phase of sprinting. Muscle forces were determined by minimizing the sum of the squares of all muscle activations. Muscle contributions to the net moments exerted about the hip, knee and ankle joints were found by multiplying the calculated value of each muscle force by the moment arm of that muscle at the joint of interest.

We calculated the actual contribution as well as the potential contribution of a muscle to the GRF. These two quantities provide different information about muscle function:

the actual contribution of a muscle to the GRF considers the magnitude of the force developed by the muscle at each instant of the simulated movement, whereas its potential contribution is independent of the muscle's force and is determined solely by the position of the body and the muscle's line-of-action at each instant. A pseudo-inverse decomposition method was used in conjunction with a ground contact model to quantify both the actual contribution of a muscle and its potential contribution to the fore-aft and vertical components of the GRF.²⁴ The ground contact model assumed that the foot contacted the ground at five discrete foot contact points. Two foot contact points were located at the medial and lateral sides of the hindfoot, two at the medial and lateral sides of the forefoot, and one at the end of the toes. A muscle's actual contribution (hereafter simply muscle contribution) was found by applying the magnitude of that muscle's force in isolation (i.e., with all other forces set to zero in the model), and using the equations for skeletal dynamics to determine its contribution to the reaction force acting at each of the five foot contact points. Similarly, a muscle's potential contribution was found by applying 1 N of muscle force in isolation, and again using the equations of skeletal dynamics to determine the contribution of this unit muscle force to the GRF.²⁵

Results for each foot contact were normalized by time (from ipsilateral foot-strike to ipsilateral toe-off) and then averaged across all participants. Fore-aft velocity (sprinting speed) was found by dividing the fore-aft displacement of the mass center by ground contact time and fore-aft acceleration was obtained by dividing the fore-aft GRF by body mass. Fore-aft and vertical GRF impulses were found by integrating each component of the GRF over the duration of the stance phase, thus:

$$\text{impulse} = \int_{t_{FS}}^{t_{TO}} \text{GRF} dt \quad (1)$$

where t_{FS} and t_{TO} represent the time of ipsilateral foot-strike and ipsilateral toe-off, respectively. Similarly, individual muscle contributions to the fore-aft and vertical GRF impulses were found by integrating each muscle's contribution to the GRF over the duration of stance. We also calculated the relative contribution of each muscle to the fore-aft and vertical GRF impulses generated at each foot contact. The relative contribution of each muscle to the fore-aft (vertical) GRF impulse was found by dividing each muscle-induced fore-aft (vertical) GRF impulse by the total muscle-induced fore-aft (vertical) GRF impulse, which was obtained by summing together all muscle-induced GRF impulses in the fore-aft (vertical) direction. This calculation was performed separately for the positive and negative contributions of each muscle to the fore-aft and vertical GRF impulses generated at each foot contact.

Each muscle's contribution to the GRF impulse was summed over all 19 foot contacts to determine its total

TABLE 1 Mean (SD) values of velocity and acceleration of the center of mass of the whole body, peak ground reaction force (GRF), and peak muscle forces for the first 19 foot contacts of the acceleration phase of sprinting

FC	Velocity (ms ⁻¹)	Acceleration (ms ⁻²)	Ground contact time (s)	Peak GRF (BW)			Peak muscle force (BW)							
				Vertical	Propulsion	Braking	ILJPSOAS	GMAX	GMED	HAMS	RF	VAS	GAS	SOL
1	3.90 (0.28)	5.78 (0.72)	0.18 (0.03)	2.17 (0.25)	0.95 (0.10)	-0.04 (0.06)	5.80 (1.26)	2.06 (0.41)	1.56 (0.50)	3.00 (0.61)	2.03 (0.54)	6.49 (2.49)	5.53 (1.08)	8.35 (1.21)
2	4.77 (0.22)	4.67 (0.66)	0.16 (0.02)	2.24 (0.23)	0.81 (0.06)	-0.06 (0.03)	6.11 (0.76)	1.91 (0.45)	2.04 (0.39)	3.42 (0.87)	2.16 (0.64)	6.78 (1.85)	5.03 (0.82)	8.53 (1.28)
3	5.50 (0.27)	4.26 (0.88)	0.15 (0.02)	2.45 (0.17)	0.83 (0.15)	-0.12 (0.11)	6.51 (0.49)	2.25 (0.07)	2.28 (0.38)	3.42 (0.83)	2.52 (0.69)	7.58 (1.76)	5.43 (0.79)	8.45 (1.42)
4	6.08 (0.29)	3.93 (0.50)	0.14 (0.02)	2.51 (0.32)	0.81 (0.05)	-0.14 (0.11)	5.80 (0.88)	2.64 (0.70)	2.08 (0.43)	3.56 (0.82)	2.12 (0.36)	7.05 (1.40)	5.16 (0.49)	8.37 (1.22)
5	6.50 (0.28)	3.80 (0.65)	0.13 (0.01)	2.96 (0.21)	0.85 (0.06)	-0.17 (0.08)	6.58 (0.38)	2.64 (0.54)	2.33 (0.50)	3.55 (0.33)	2.28 (0.35)	7.23 (1.17)	5.67 (1.00)	10.67 (1.12)
6	6.98 (0.37)	3.47 (0.67)	0.13 (0.01)	2.80 (0.37)	0.81 (0.04)	-0.18 (0.11)	6.64 (1.12)	2.89 (1.38)	2.62 (0.36)	4.21 (1.38)	2.35 (0.67)	7.00 (0.47)	4.65 (0.59)	9.64 (1.06)
7	7.31 (0.41)	2.96 (0.64)	0.12 (0.01)	3.08 (0.17)	0.81 (0.08)	-0.28 (0.09)	6.68 (0.98)	2.82 (1.23)	2.86 (0.66)	3.93 (1.32)	2.78 (0.67)	7.78 (0.76)	4.88 (0.51)	10.03 (1.43)
8	7.59 (0.46)	2.52 (0.43)	0.12 (0.01)	2.94 (0.29)	0.78 (0.04)	-0.28 (0.08)	6.53 (0.48)	2.61 (1.26)	2.31 (0.39)	3.88 (0.95)	2.00 (0.29)	6.93 (0.61)	5.20 (1.01)	9.92 (1.67)
9	7.73 (0.54)	2.24 (0.66)	0.12 (0.01)	3.17 (0.22)	0.78 (0.10)	-0.34 (0.05)	6.19 (0.71)	2.22 (0.76)	2.11 (0.71)	3.51 (0.94)	2.52 (0.34)	6.55 (2.91)	5.10 (0.55)	10.52 (1.33)
10	7.91 (0.58)	2.02 (0.62)	0.12 (0.01)	3.18 (0.31)	0.76 (0.07)	-0.34 (0.10)	5.67 (1.29)	2.31 (1.10)	2.35 (0.37)	3.42 (0.63)	2.04 (0.59)	7.43 (2.11)	4.40 (0.63)	9.68 (1.22)
11	8.09 (0.56)	1.81 (0.37)	0.11 (0.01)	3.33 (0.25)	0.75 (0.07)	-0.42 (0.04)	6.48 (0.41)	2.16 (0.74)	2.44 (0.54)	3.07 (0.67)	2.13 (1.14)	7.25 (2.70)	4.18 (0.69)	10.38 (1.05)
12	8.26 (0.62)	1.63 (0.59)	0.12 (0.01)	3.27 (0.43)	0.74 (0.06)	-0.39 (0.14)	6.21 (1.11)	2.69 (0.92)	2.87 (0.59)	3.55 (0.85)	2.17 (0.82)	7.36 (1.92)	3.99 (0.57)	9.04 (1.80)
13	8.28 (0.61)	1.72 (0.75)	0.11 (0.01)	3.41 (0.16)	0.75 (0.06)	-0.43 (0.13)	5.91 (0.94)	2.46 (0.78)	2.77 (0.28)	3.28 (0.86)	2.81 (1.52)	5.34 (2.51)	4.70 (0.66)	9.65 (1.55)
14	8.46 (0.62)	1.47 (0.46)	0.11 (0.01)	3.35 (0.25)	0.71 (0.10)	-0.41 (0.12)	6.44 (0.22)	2.45 (1.02)	2.84 (0.49)	3.56 (0.64)	2.13 (0.62)	6.57 (0.97)	3.50 (0.70)	9.41 (1.49)
15	8.56 (0.63)	1.00 (0.19)	0.11 (0.01)	3.45 (0.25)	0.70 (0.04)	-0.51 (0.05)	6.69 (0.55)	2.71 (0.85)	3.00 (0.58)	3.25 (0.46)	2.80 (1.01)	7.21 (3.49)	4.23 (0.55)	10.35 (1.02)
16	8.65 (0.69)	1.26 (0.48)	0.11 (0.01)	3.37 (0.23)	0.72 (0.06)	-0.43 (0.20)	5.67 (1.67)	2.58 (0.90)	2.71 (0.60)	3.65 (1.31)	2.25 (1.10)	6.01 (1.78)	3.96 (0.69)	9.49 (1.49)
17	8.72 (0.73)	1.14 (0.43)	0.10 (0.01)	3.58 (0.36)	0.72 (0.06)	-0.52 (0.10)	6.42 (0.34)	2.47 (0.68)	2.93 (0.28)	3.04 (0.55)	3.21 (1.67)	5.70 (2.74)	4.47 (0.47)	10.23 (2.17)
18	8.93 (0.59)	1.16 (0.87)	0.10 (0.01)	3.42 (0.33)	0.71 (0.06)	-0.52 (0.15)	6.63 (0.74)	3.30 (0.58)	3.10 (0.73)	3.61 (1.01)	2.90 (2.25)	6.79 (2.45)	4.64 (1.25)	8.97 (1.57)
19	9.05 (0.66)	1.41 (0.14)	0.11 (0.01)	3.61 (0.41)	0.75 (0.05)	-0.51 (0.07)	6.90 (0.94)	3.33 (0.62)	2.73 (0.39)	4.00 (1.05)	2.57 (0.65)	6.62 (0.47)	4.56 (1.55)	8.77 (1.54)

Peak GRF is represented by the peak vertical, propulsive, and braking components. Peak GRF and muscle forces for each participant were normalized by body weight and the results then averaged across all participants.

Abbreviations: BW, body weight; FC, foot contact. Muscle symbols are as follows: GAS, medial and lateral compartments of gastrocnemius combined; GM·AX, superior, middle, inferior portions of gluteus maximus combined; GMED, anterior, middle and posterior portions of gluteus medius combined; HAMS, semimembranosus, semitendinosus, biceps femoris long head, biceps femoris-short head combined; ILIOPSOAS, iliacus and psoas combined; RF, rectus femoris; SOL, soleus; VAS, vastus medialis, intermedius, and lateralis combined.

contribution over the acceleration phase. This summation was done for the fore-aft and vertical GRF impulses separately. Using these data, we then classified each muscle as a “supporter” and/or “accelerator/brake.” A muscle was classified as a “supporter” if its total contribution to the vertical GRF impulse was positive (i.e., overall it delivered an upward impulse to the body). A muscle was classified as an “accelerator” if its total contribution to the fore-aft GRF impulse was positive (i.e., overall it generated a propulsive impulse that increased forward momentum of the body), and it was classified as a “brake” if its contribution to the fore-aft GRF impulse was negative (i.e., overall it generated a backward impulse that retarded forward momentum of the body). For illustrative purposes, results are presented for the 1st, 7th, and 19th foot contacts (FC1, FC7, FC19), as these represent high-, medium- and low-acceleration conditions, respectively.

3 | RESULTS

The velocity of the center of mass at FC1 (3.90 ± 0.28 m/s) was nearly doubled at FC7 (7.31 ± 0.41 m/s) and increased gradually over the next 12 foot contacts to reach a maximum of 9.05 ± 0.66 m/s at FC19 (Figure S1 and Table 1). Maximum acceleration occurred at FC1 (5.78 ± 0.72 m/s²) and was nearly halved by FC7 (2.96 ± 0.64 m/s²) before decreasing to 1.41 ± 0.14 m/s² at FC19. The peak vertical GRF increased by 66% from FC1 to FC19 (Table 1). The peak positive fore-aft GRF (i.e., propulsive force) decreased by 15% over the first 7 foot contacts and remained roughly constant thereafter, whereas the absolute magnitude of the peak negative fore-aft GRF (i.e., braking force) increased steadily with sprinting speed.

Gluteus maximus developed peak forces during early stance whereas vasti and soleus forces peaked near mid-stance (Figure 1). Gastrocnemius and rectus femoris forces peaked during the second half of stance while the force in iliopsoas increased sharply just before toe-off. The forces in gluteus medius, hamstrings and rectus femoris varied less throughout stance. The mean peak force in soleus ranged from 8.4 to 10.7 body weight (BW) across all foot contacts while that in vasti was less (5.3–7.8 BW) (Table 1). Mean peak forces in the hamstrings, gluteus maximus, and gluteus medius were even lower and ranged from 3.0–4.2 BW, 2.0–3.3 BW, and 1.6–3.1 BW, respectively, throughout the acceleration phase.

Gluteus maximus and the hamstrings were the major contributors to the extensor moment exerted about the hip during the first half of stance while iliopsoas and rectus femoris contributed the bulk of the hip flexion moment during the second half of stance (Figure 2). The hamstrings applied a peak hip extensor moment of 1.3 ± 0.4 Nm/kg at FC1 compared to 1.2 ± 0.2 Nm/kg for gluteus maximus. The peak hip flexion

moment applied by iliopsoas reached 1.9 ± 0.2 Nm/kg at FC19. The vasti and rectus femoris were major contributors to the extension moment developed about the knee, with the hamstrings and gastrocnemius applying relatively large knee flexion moments throughout stance. The vasti produced a peak knee extensor moment of 2.9 ± 0.2 Nm/kg, considerably higher than the moment exerted by any other muscle at the knee (Figure 2, FC19). Interestingly, rectus femoris and hamstrings applied nearly equal and opposite moments about the knee at all foot contacts. Soleus and gastrocnemius combined to produce most of the plantarflexion moment generated at the ankle, with the moment due to soleus being larger for most of the stance phase. At FC19, soleus applied a peak plantarflexion moment of 2.7 ± 0.4 Nm/kg compared to 1.5 ± 0.4 Nm/kg from gastrocnemius. The net moments exerted by the muscles crossing the hip, knee and ankle in the model were practically equivalent to the net joint moments calculated from inverse dynamics: mean RMS differences were less than 0.2 Nm/kg, 0.05 Nm/kg, and 0.04 Nm/kg for the hip, knee, and ankle, respectively (cf. dashed black lines and shaded areas in Figure 2).

Gastrocnemius generated the highest propulsive force of any muscle at all foot contacts (Figure 3A). Gastrocnemius' peak propulsive force was maximum at FC1 (0.58 ± 0.08 BW) and decreased steadily to reach 0.47 ± 0.10 BW at FC19. Soleus also generated substantial propulsive forces during the first few steps (e.g., peak of 0.46 ± 0.08 BW at FC1), after which this muscle induced a braking force during the first half of stance that increased in magnitude with running speed. The hamstrings generated peak propulsive forces of ~ 0.15 BW during the first half of stance at all foot contacts. Gluteus maximus also contributed to propulsion during the first half of stance, but only from FC1 to FC7, and its overall contribution was relatively small. Gluteus medius generated a propulsive force of ~ 0.06 BW throughout the stance phase at all foot contacts. The vasti, rectus femoris and iliopsoas induced braking forces during the stance phase at all foot contacts. The peak braking force applied by the vasti increased with running speed and reached 0.58 ± 0.11 BW at FC19. The braking force induced by iliopsoas was small (not shown in Figure 3A). The vasti acted synergistically with soleus and gastrocnemius to generate a support force throughout stance whereas the hamstrings and iliopsoas accelerated the body downward (Figure 3B). Soleus induced a peak support force of 1.61 ± 0.18 BW at FC19 compared to 0.71 ± 0.26 BW and 0.56 ± 0.07 BW for gastrocnemius and the vasti, respectively.

The gluteals, hamstrings, and ankle plantarflexors displayed potential to generate a propulsive impulse and increase forward momentum of the body at all foot contacts (Figure 4A). Gastrocnemius and the hamstrings had the highest potential to generate a propulsive impulse, followed by gluteus medius and soleus. The vasti, rectus femoris and

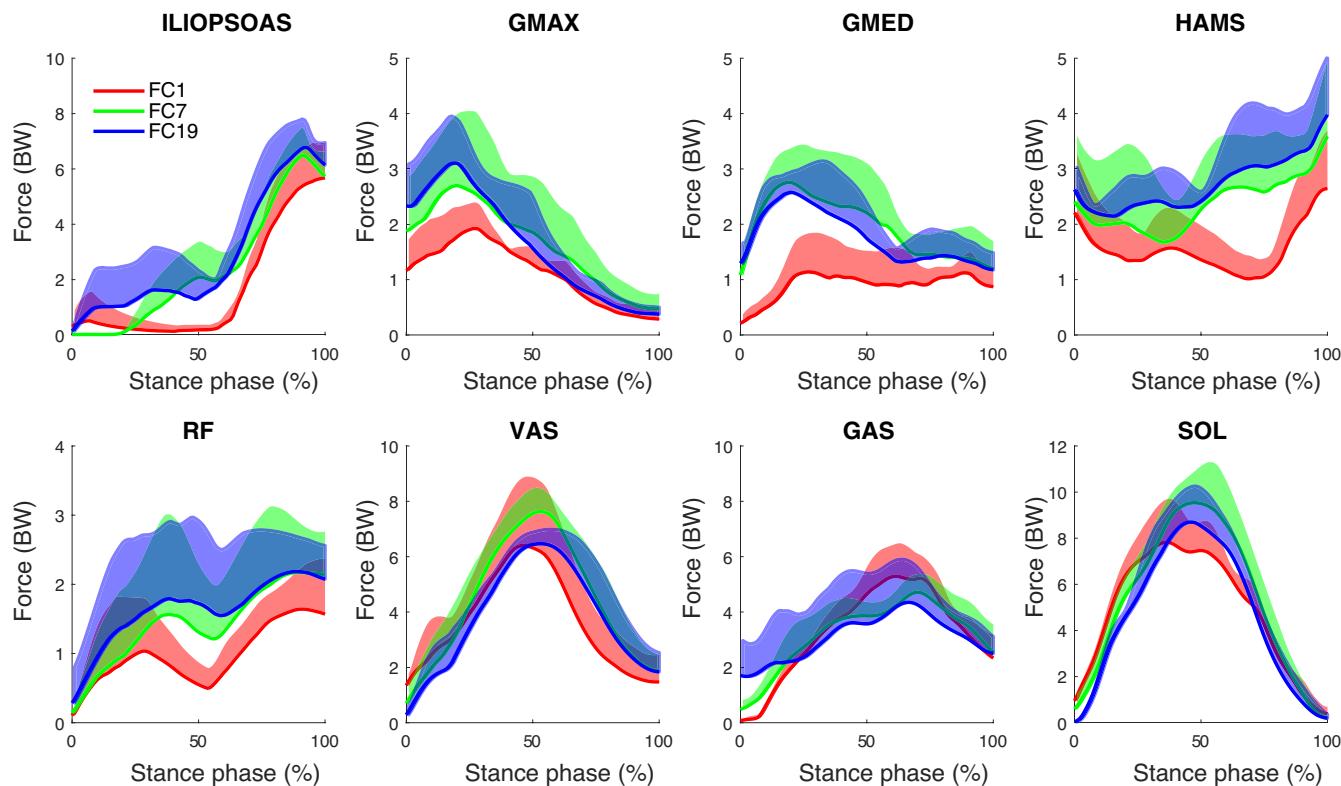


FIGURE 1 Time histories of the forces calculated for representative muscles at the 1st, 7th and 19th foot contacts (FC1, FC7 and FC19) of the acceleration phase of sprinting. The solid lines represent mean muscle forces for all participants and the shaded areas represent ± 1 standard deviation from the mean. Muscle forces were normalized by each participant's body weight (BW). Muscle symbols are: ILIOPSOAS, iliacus and psoas combined; GMAX, superior, middle, inferior portions of gluteus maximus combined; GMED, anterior and posterior portions of gluteus medius/minimus combined; HAMS, semimembranosus, semitendinosus, and biceps femoris long head and short head combined; RF, rectus femoris; VAS, vastus medialis, intermedius, and lateralis combined; SOL, soleus; GAS, medial and lateral gastrocnemius combined. Results shown are for the ipsilateral limb

iliopsoas had potential to induce braking impulses and retard forward momentum at all foot contacts. All the major muscles of the lower limb, except the hamstrings and iliopsoas, showed potential to generate an upward (support) impulse during the acceleration phase (Figure 4B). The vasti and gastrocnemius displayed the highest potential to generate a support impulse, followed by soleus. The gluteals displayed less potential to generate a support impulse than the vasti and the ankle plantarflexors. The hamstrings and iliopsoas each had potential to induce a negative vertical impulse, reflecting their ability to accelerate the mass center downward.

The net vertical impulse was approximately 2.5 times greater than the net fore-aft impulse at FC1 and up to 15 times greater at FC19 (Figure 5, GRF). The net fore-aft impulse remained positive (i.e., the propulsive impulse was greater than the braking impulse) across all 19 foot contacts. It decreased by 65% over the first 7 foot contacts and fell more gradually thereafter. The net vertical impulse was also positive (support) across all 19 foot contacts, but it remained relatively constant because an increase in the magnitude of the vertical GRF was offset by a decrease in ground contact time (see Table 1).

Gastrocnemius, soleus, hamstrings, and the gluteal muscles functioned as accelerators while the vasti and rectus femoris acted as brakes (Figure 5A, bottom panel). Gastrocnemius and soleus were the major accelerators, as these muscles contributed substantially to the propulsive impulse generated over all 19 foot contacts (Figure 5A, top). The hamstrings and gluteals generated much smaller propulsive impulses than the ankle plantarflexors during the first 10 steps (FC1 to FC10), but their contributions to forward propulsion were more consistent in magnitude over all 19 steps. Gastrocnemius, soleus and the hamstrings contributed 37%, 23% and 15%, respectively, of the total propulsive impulse generated by all the muscles over all 19 foot contacts, whereas the contributions from gluteus medius and gluteus maximus were only 7% and 2%, respectively (Figure 5A, bottom). The vasti and rectus femoris induced braking impulses that retarded forward momentum at all foot contacts, with vasti's contribution being much greater (53% for VAS and 15% for RF).

Soleus, gastrocnemius, vasti, rectus femoris and the gluteal muscles acted as supporters (Figure 5B). Soleus was the major supporter, contributing 44% of the total upward (support) impulse generated by all the muscles over all 19 foot

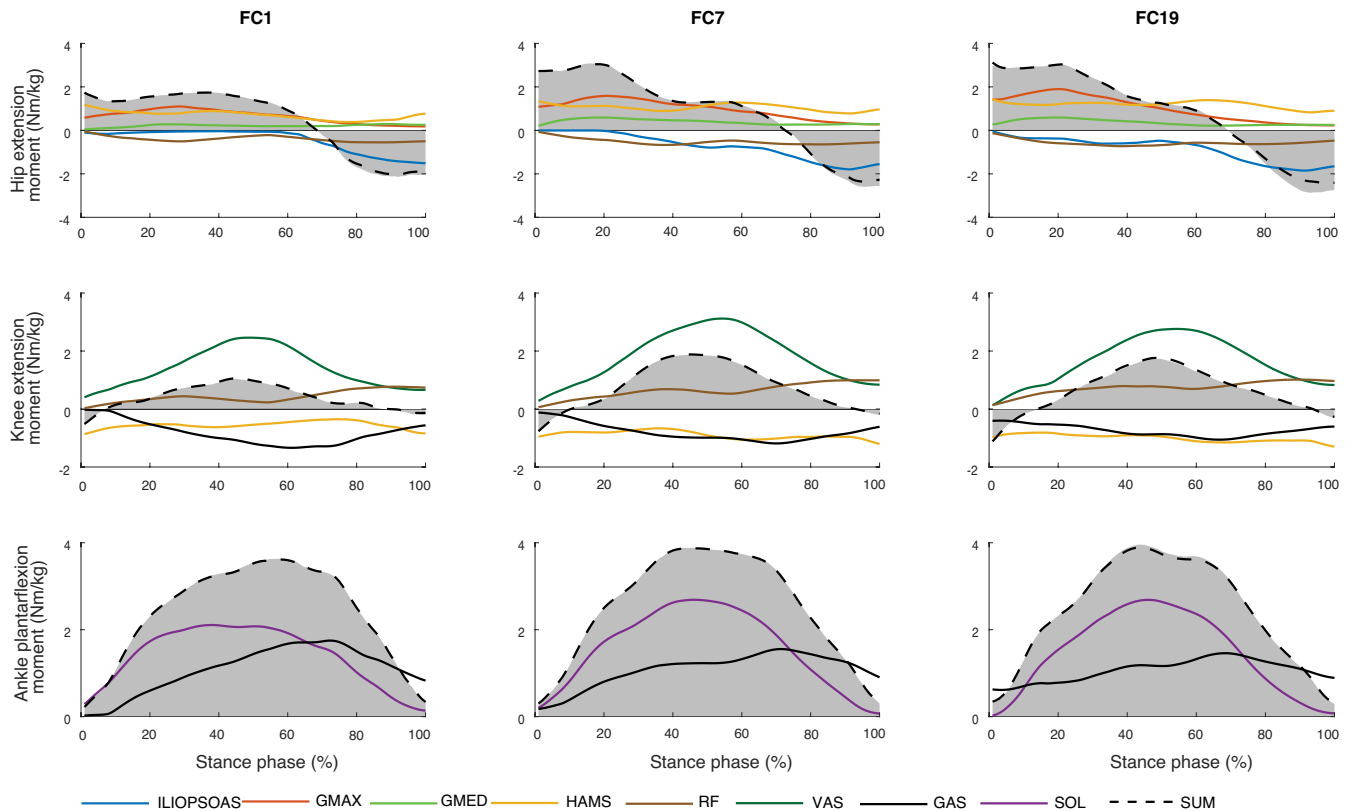


FIGURE 2 Contributions of individual muscles to the net joint moments exerted about the hip, knee, and ankle for the 1st, 7th and 19th foot contacts (FC1, FC7 and FC19). Moments were normalized by each participant's body mass and averaged across all participants. The shaded regions represent the net joint moments calculated from the experimental gait data using inverse dynamics while the dashed lines are the model-predicted moments obtained by taking the product of muscle force and moment arm and summing across all the muscles spanning each joint. Hip extension, knee extension and ankle plantarflexion moments are positive. Muscle symbols are defined in Figure 1

contacts (Figure 5B, bottom). The gastrocnemius and vasti also contributed substantially to the support impulse, with these muscles generating 21% and 17%, respectively. Rectus femoris, gluteus maximus and gluteus medius contributed less to the support impulse than either of the ankle plantarflexors and vasti. The hamstrings and iliopsoas induced negative vertical impulses, consistent with their tendency to accelerate the body downward (see Figure 4). Iliopsoas was the only muscle to accelerate the body backward and downward at all foot contacts, but its overall contribution to the GRF impulse was negligible (not shown). The hamstrings and rectus femoris generated GRF impulses that were diametrically opposed: the hamstrings induced fore-aft and vertical impulses that were directed forward and downward, respectively, whereas those from rectus femoris were directed backward and upward (cf. HAMS and RF in Figure 5).

The ankle plantarflexors, soleus and gastrocnemius, dominated the net fore-aft (propulsive) impulse for the entire acceleration phase, with their contributions being ~ 0.2 Ns/kg greater than the total propulsive impulse generated over all 19 foot contacts except at FC1 (Figure 6A). The hamstrings and gluteals also contributed substantially to the net

fore-aft impulse. The combined effect of the vasti and rectus femoris was a braking impulse induced at all foot contacts. Soleus, gastrocnemius, vasti and rectus femoris generated practically all the net vertical (support) impulse at each step (Figure 6B).

4 | DISCUSSION

We quantified the contributions of individual lower-limb muscles to the vertical and fore-aft GRF impulses generated for the majority of the acceleration phase (19 foot contacts) of a maximal sprint. The ankle plantarflexors played a major role in generating the support and increase in forward momentum needed to progress sprinting speed toward upper limits (Figures 3 and 5). Soleus acted primarily as a supporter and provided a substantial fraction of the upward impulse at each foot contact. Gastrocnemius generated most of the propulsive impulse but also contributed to the upward impulse and therefore functioned as both an accelerator and supporter. The hamstrings and gluteus medius developed extensor moments about the hip and functioned primarily as accelerators by contributing appreciably to the increase in

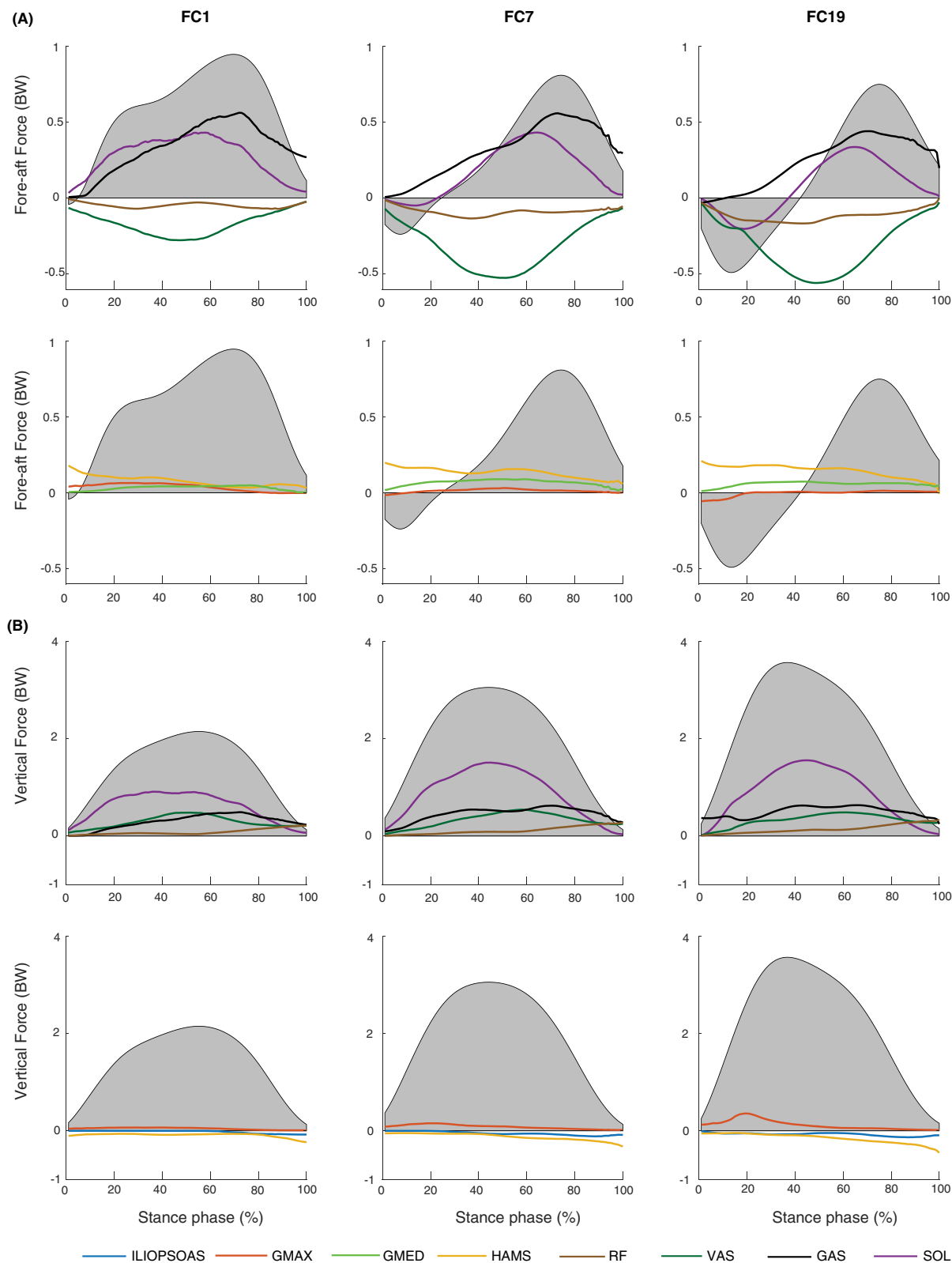


FIGURE 3 Contributions of individual muscles to the fore-aft (A, top two rows) and vertical (B, bottom two rows) components of the GRF for the 1st, 7th and 19th foot contacts (FC1, FC7 and FC19). GRFs were normalized by each participant's body weight (BW) and averaged across all participants. The shaded regions represent the force plate measurements obtained at each foot contact. Muscle symbols are defined in Figure 1

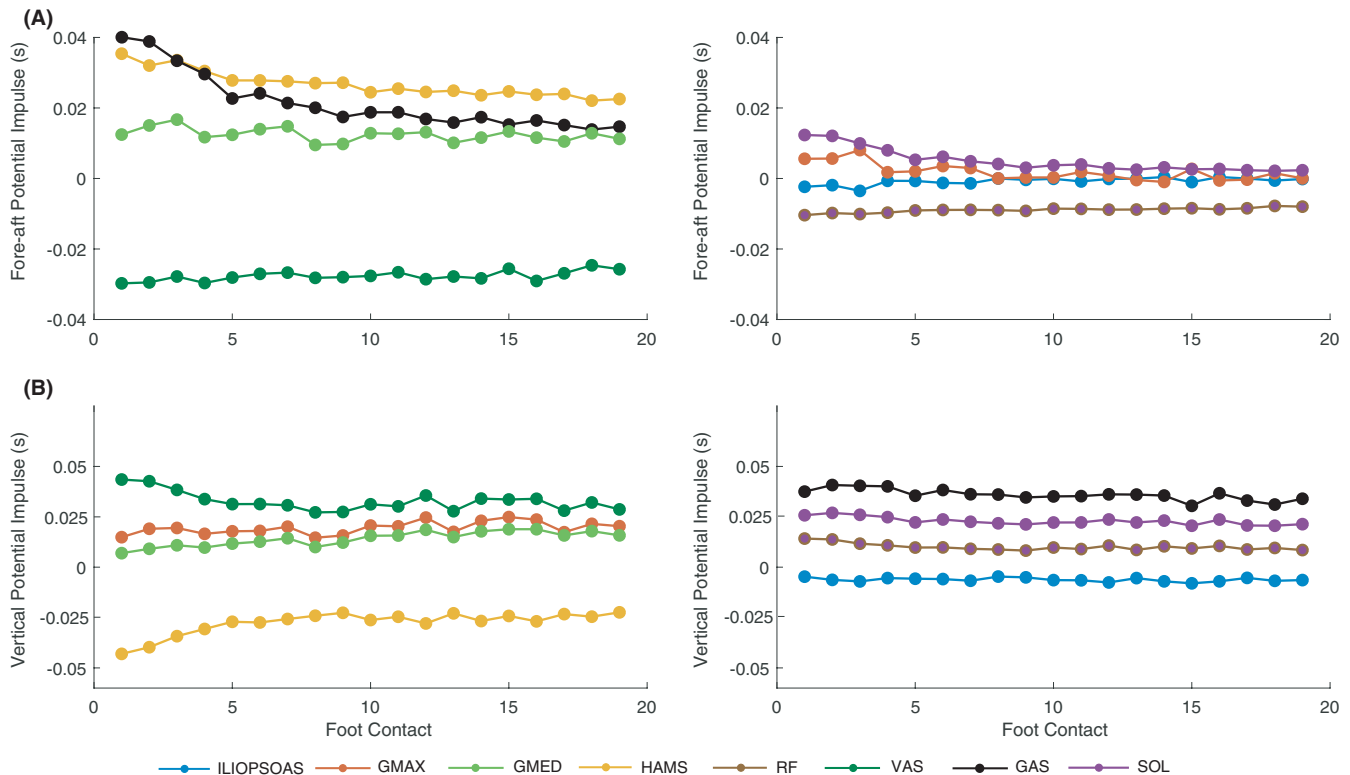


FIGURE 4 Potential muscle contributions to the fore-aft (A) and vertical (B) GRF impulses for the first 19 foot contacts of the acceleration phase of sprinting. The potential contribution of a muscle to the GRF impulse represents the effect of a unit of force (1.0 N) applied by that muscle in isolation, with all other muscle forces assumed to be zero at that instant. Potential muscle contributions to the GRF impulse were normalized by body mass and averaged across all participants. Muscle symbols are defined in Figure 1

forward momentum of the body; however, the hamstrings also accelerated the body downward and detracted from support. The vasti and rectus femoris functioned primarily as supporters, but these muscles also retarded forward momentum at each foot contact and acted as brakes. Gluteus maximus contributed relatively little to either the propulsive or support impulse. Overall, the ankle plantarflexors and hip extensors/abductors functioned as accelerators whereas the knee extensors acted as a brake (Figure 6). The ankle plantarflexors and knee extensors generated nearly all of the support impulse at each foot contact.

We combined computational modeling of the human musculoskeletal system and experimental data to determine the forces developed by the individual muscles of the lower limb and their contributions to the GRF impulse during the stance phase of maximum acceleration sprinting. This approach has been used previously to quantify muscle function in other activities; for example, to determine muscle contributions to the acceleration of the body's center of mass during walking²⁶ and running,³ as well as the contributions of individual muscles to the contact forces transmitted by the hip and knee during gait.^{27,28} In these studies, muscle EMG data were compared to model-predicted muscle forces to verify the model calculations, although more direct methods are also available for monitoring muscle-tendon forces in vivo.^{29,30} The results of

these studies lend confidence to the belief that computational modelling offers a valid and practical approach for better understanding muscle function during movement.

Our results are consistent with those reported previously by others. The mean forward acceleration of the mass center was 5.78 m/s^2 at FC1 compared to 1.41 m/s^2 at FC19, while the corresponding forward velocities were 3.90 m/s and 9.05 m/s , respectively (Table 1 and Figure S1). This spectrum of speed and acceleration is comparable to that measured for well-trained sprinters.^{2,31,32} Our estimates of muscle function for sprinting at a speed of approximately 9.0 m/s in the present study are also comparable to results obtained by Dorn et al.² for a similar cohort of highly trained athletes sprinting at a speed of 9.5 m/s . For example, these authors found that soleus, gastrocnemius and the vasti contributed the bulk of the support force generated by the lower-limb muscles during steady-state sprinting, consistent with our findings here.

Soleus contributed more substantially to support than gastrocnemius, but our analyses indicate that gastrocnemius was more important for increasing forward momentum of the body at all foot contacts. The reason soleus delivered a larger upward impulse than gastrocnemius even though gastrocnemius had greater potential for generating support (Figures 4B and 5B) is because the force developed by soleus was considerably higher for most of the stance phase (Figure 1).

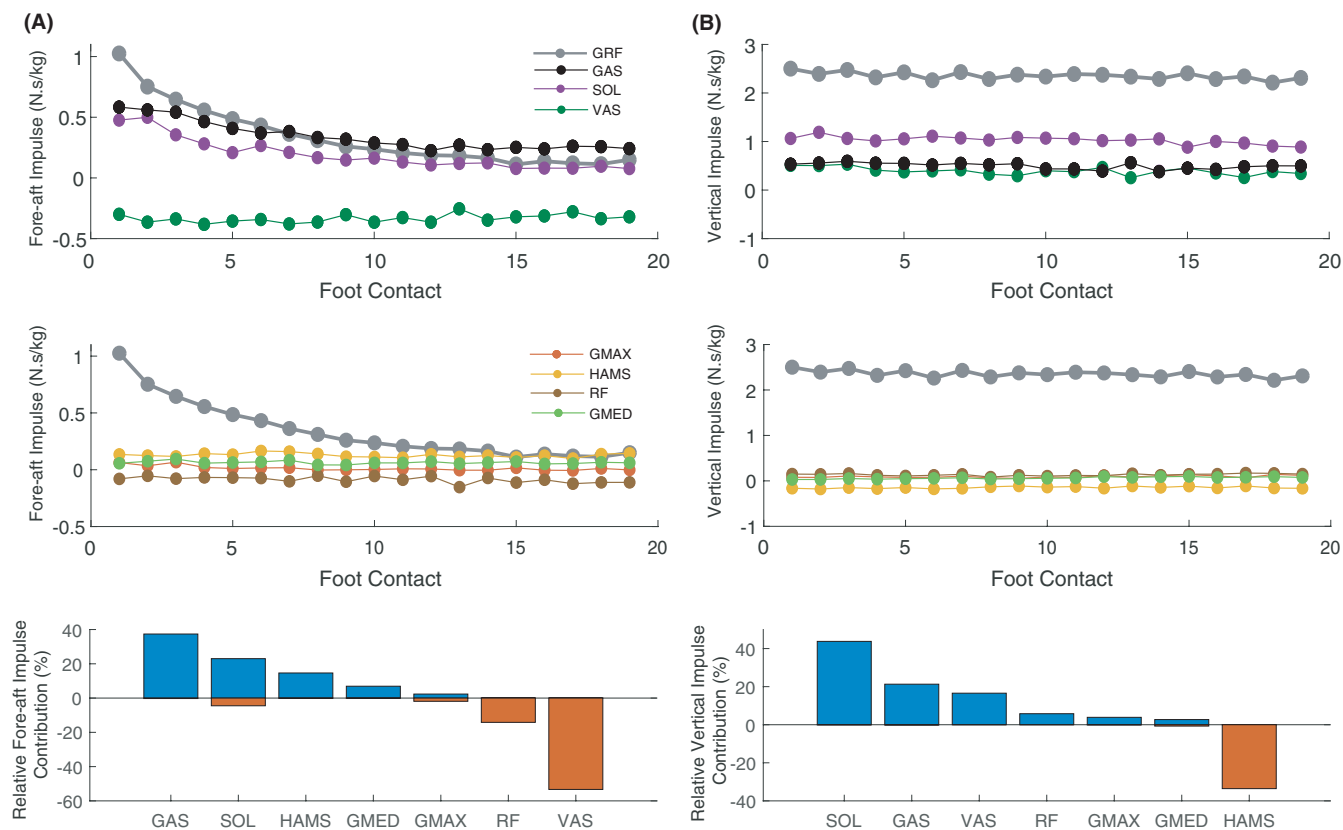


FIGURE 5 Actual muscle contributions to the net fore-aft (A) and vertical (B) GRF impulses for the first 19 foot contacts of the acceleration phase of sprinting. The actual contribution of a muscle considers the magnitude of force developed by that muscle at each instant of the simulated sprint. The top two rows show the muscle contributions to net fore-aft (propulsive) and vertical (support) GRF impulses generated at each foot contact. The bottom row shows the percentage contributions of individual muscles to the total propulsive and support GRF impulses generated by all the muscles across all 19 foot contacts. Muscle contributions to the GRF impulse were normalized by body mass and averaged across all participants. Muscle symbols are defined in Figure 1

Importantly, soleus induced a relatively large braking force during the first half of stance from FC7 onward whereas gastrocnemius accelerated the center of mass forward for almost the entire stance phase at all foot contacts (Figure 3A, compare GAS and SOL at FC1, FC7 and FC9). This behavior was critical to maximizing the increase in forward momentum of the body, and it explains why the propulsive impulse generated by gastrocnemius remained larger than that due to soleus throughout the acceleration phase (Figure 5A). We conclude that the two major plantarflexors, soleus and gastrocnemius, have distinct roles in optimizing performance during maximum acceleration sprinting: soleus accounted for a large fraction of the upward impulse generated at each foot contact and acted primarily as a supporter, whereas gastrocnemius contributed markedly to the propulsive and upward impulses and functioned as both accelerator and supporter.

While the ankle plantarflexors (and especially gastrocnemius) were the major contributors to the propulsive impulse generated across all foot contacts (Figure 5A), our calculations suggest that the hamstrings are also important for increasing speed when commencing a sprint from a stationary position. The hamstrings contributed substantially to the

propulsive impulse because these muscles displayed a high potential to accelerate the body forward at all foot contacts (Figure 4A) and because they applied relatively high forces (mean magnitudes $\sim 1\text{--}3$ BW) throughout the stance phase (Figure 1). These results are consistent with those of Debaere et al.¹⁷ who found that the hamstrings (specifically biceps femoris long head) assisted in accelerating the body forward during the first foot contact after block clearance.

Morin et al.³³ noted that the net fore-aft (propulsive) GRF impulse was greater during the first few steps in world-class sprinters than in high-level sprinters, implying that sprinting performance depends on the magnitude of the propulsive impulse generated at the beginning of the acceleration phase. In a related study, these same investigators found that higher propulsive forces generated during the first 10 foot contacts of a maximal sprint on an instrumented treadmill correlated with increased biceps femoris muscle activity during terminal swing, hence they concluded that the hamstrings play a major role in increasing forward momentum of the body during the first few foot contacts of accelerated sprinting.¹⁴ Our calculations show that the propulsive impulse is high during the first few foot contacts of the acceleration phase because of

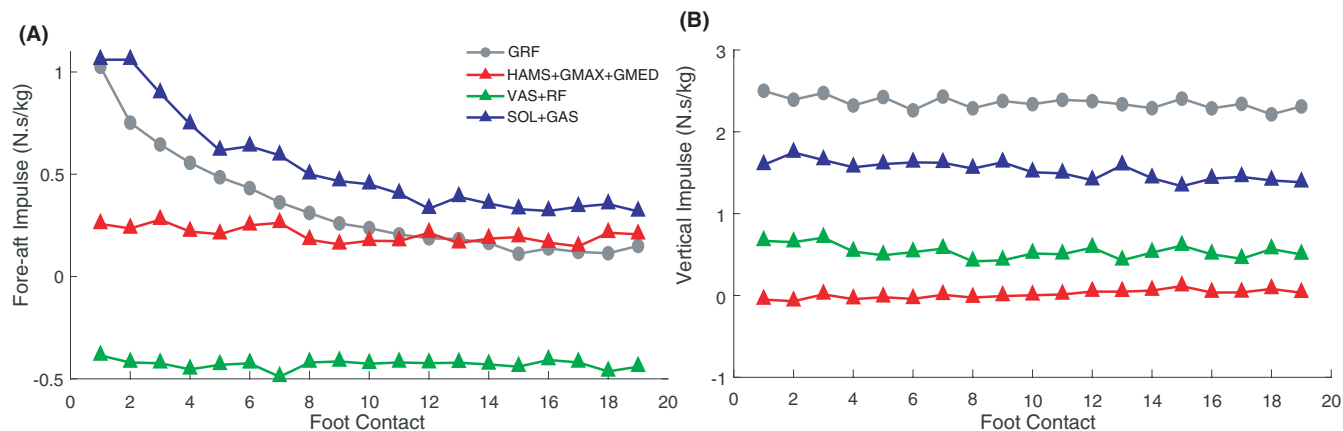


FIGURE 6 Contributions of the hamstrings, gluteus maximus and gluteus medius combined (HAMS + GMAX + GMED), vasti and rectus femoris combined (VAS + RF), and soleus and gastrocnemius combined (SOL + GAS) to the fore-aft GRF impulse (A) and the vertical GRF impulse (B) across all 19 foot contacts of the acceleration phase. GRF represents the net impulse delivered to the ground in the vertical and fore-aft directions; specifically, net fore-aft impulse = propulsive impulse – braking impulse, and net vertical impulse = upward impulse – downward impulse. Muscle symbols are defined in Figure 1

the contributions of gastrocnemius and soleus more so than hamstrings. Gastrocnemius and soleus both delivered relatively large propulsive impulses over the first 3–4 foot contacts whereas hamstrings' contribution was more uniform throughout the acceleration phase (Figure 5A). We conclude that the ankle plantarflexors play a major role in accelerating the body forward during the first few foot contacts and that hamstrings' contribution becomes relatively more important as sprinting speed progresses toward upper limits.

Descriptions of gluteus maximus function during running and sprinting are somewhat inconsistent in the literature. EMG measurements indicate that gluteus maximus has little or no activity in upright standing and walking, and that this muscle is primarily active during running and in other tasks that require the trunk to be stabilized against flexion.³⁴ Lieberman et al.¹⁶ found a strong correlation between peak EMG activity of gluteus maximus on the stance side and peak amplitude of trunk pitch velocity at relatively low running speeds (2.0–4.0 m/s). They concluded that a major role of gluteus maximus is to extend the hip on the stance side to control trunk flexion during running. Bartlett et al.¹⁵ found that gluteus maximus' activity during running at 5.3 m/s was much greater than at 3.0 m/s, but that only the inferior portion of this muscle responded to changes in trunk pitch velocity. These authors concluded that gluteus maximus has a limited role in controlling trunk flexion during running. Our calculations indicate that gluteus maximus' contribution to the propulsive impulse was minimal throughout the acceleration phase (Figure 5A, GMAX). Gluteus maximus developed a mean peak force ranging from 1.9 to 3.5 BW (Figure 1 and Table 1), contributed considerably to the net extension moment exerted about the hip (Figure 2), and accelerated the hip into extension with much vigor at all foot contacts (see Figure S2). Gluteus maximus' contribution to

the propulsive impulse was small because it displayed a relatively low potential to generate a propulsive GRF impulse at all foot contacts (Figure 4A, GMAX). The hamstrings also applied a large extensor moment about the hip and accelerated the hip into extension at all foot contacts (Figure S2). In contrast to gluteus maximus, however, the hamstrings contributed significantly to the propulsive impulse and increase in forward momentum of the body (Figure 5A, cf. HAMS and GMAX). These results suggest that gluteus maximus plays a limited role in accelerating the body toward peak sprinting speed.

If gluteus maximus contributes little to the GRF impulse during accelerated sprinting, why is this muscle group so well developed in elite sprinters? Miller et al.³⁵ used magnetic resonance imaging to measure lower-limb muscle volumes in 5 elite sprinters, 26 sub-elite sprinters, and 11 untrained controls. They found the relative volume of gluteus maximus (normalized by body mass) for elite sprinters to be 25% and 67% larger than that for sub-elite sprinters and untrained controls, respectively. Further, the relative volume of gluteus maximus alone explained 33.6% of the variance in performance among sprinters,³⁵ indicating that this muscle group is important for maximizing sprinting performance. To further examine the role of gluteus maximus in accelerated sprinting, we calculated the force developed by this muscle group and its contribution to hip-joint acceleration during the swing phase of the sprinting cycle at each of the 19 foot contacts (Figure S3). The hamstrings and gluteus maximus developed relatively high peak forces during the terminal swing phase (Figure S3A; at FC19, HAMS force peaked at ~8 BW whereas GMAX force peaked at ~4.5 BW). These muscles contributed significantly to accelerating the hip into extension throughout the swing phase and especially during terminal swing

(Figure S3B). Thus, while gluteus maximus contributed relatively little to the GRF impulse, this muscle, with assistance from the hamstrings, was responsible for extending the hip and decelerating the swinging leg in preparation for foot contact at the next step. These results are consistent with those reported for steady-speed sprinting, where gluteus maximus and the hamstrings were found to play a major role in increasing stride frequency by accelerating the hip into extension during terminal swing.^{2,3} Therefore, larger gluteus maximus muscle volumes in elite sprinters may not be a consequence of stance phase force production; instead, we suggest this morphological feature could be explained by the need to maintain a high stride frequency during the swing phase of each step.¹¹

Relatively little is known about the role of gluteus medius in running and sprinting. Bartlett et al.¹⁵ found that EMG activity of gluteus medius is significantly greater for running at a constant speed of 5.3 m/s compared to 3.0 m/s. Simulation studies have shown that gluteus medius contributes moderately to support and propulsive forces generated while running at different steady-state speeds.^{2,3} Our analysis suggests that gluteus medius functions primarily as an accelerator in high-speed sprinting. This muscle contributed noticeably to the propulsive impulse generated across all 19 foot contacts but relatively little to the support impulse (Figure 5, GMED). Similar to the actions of the hamstrings and gluteus maximus, gluteus medius exerted an extensor moment about the hip and accelerated the hip into extension, albeit to a lesser extent for most of the stance phase (Figure 2 and Figure S2). Gluteus medius' contribution to the propulsive impulse was lower than that from the hamstrings at all foot contacts, but its contribution to the propulsive impulse generated over all 19 steps was nonetheless important (Figure 5A, GMED). Gluteus medius contributed substantially to an increase in forward momentum mainly because its potential to generate a propulsive GRF impulse remained relatively high at all foot contacts (Figure 4A).

The vasti functioned as a supporter and brake at each foot contact of the acceleration phase (Figure 5). The vasti acted synergistically with soleus and gastrocnemius to accelerate the body upward and simultaneously induced a large braking force that retarded forward momentum of the body. However, these muscles displayed another important function in controlling motion of the center of mass in the mediolateral direction. As sprinting speed progressed toward upper limits, the vasti not only generated higher support and braking forces (Figure 3), this muscle group also transmitted medially-directed forces to the ground (see Figure S4). These medial ground forces helped to stabilize the mediolateral motion of the body by counter-balancing the large lateral forces transmitted to the ground by soleus and gastrocnemius. These results may be contrasted with those found for walking, where the vasti act in concert with the ankle plantarflexors (soleus and gastrocnemius) to accelerate the body laterally while

gluteus medius actively controls balance by accelerating the body medially.²⁶ In accelerated sprinting, the vasti act synergistically with gluteus medius and rectus femoris to stabilize mediolateral motion of the center of mass (Figure S4). Thus, while the primary role of the vasti as a supporter was to accelerate the body upward during stance, this muscle group also retarded running speed (i.e., functioned as a brake) and, along with gluteus medius and rectus femoris, controlled mediolateral balance.

In their analyses of muscle mechanical power during explosive movements such as jumping and sprinting, Jacobs et al.³⁶ found that rectus femoris transferred power from the hip to the knee whereas the hamstrings transferred power in the opposite direction, from the knee to the hip. The outcome was a net transfer of power from the hip to the knee joint, which enhanced performance. This result parallels our finding here of opposing actions of these two biarticular muscles in relation to the forces transmitted to the ground. Rectus femoris and the hamstrings acted antagonistically at each foot contact throughout accelerated sprinting, with the former contributing to support and the latter accelerating the body downward (Figures 3B and 5B). In the fore-aft direction, the hamstrings contributed considerably to forward propulsion, especially during early stance, whereas rectus femoris induced a braking force throughout stance; and in the mediolateral direction, the hamstrings accelerated the body laterally whereas rectus femoris induced a medial acceleration (Figure S4). Future work should aim to reconcile these findings by accounting for muscle-induced accelerations in analyses of mechanical power generation and transfer during sprinting.

In a recent study, Schache et al.¹³ investigated the stance phase mechanical function of sagittal-plane hip, knee, and ankle moments during maximum acceleration sprinting. They analyzed three distinct phases based on the magnitude of the average forward acceleration of the body's center of mass: high acceleration phase of $5.30 \pm 0.64 \text{ m/s}^2$ (FC1 and FC2); medium acceleration phase of $2.93 \pm 0.14 \text{ m/s}^2$ (FC5 to FC9); and low-acceleration phase of $1.32 \pm 0.11 \text{ m/s}^2$ (FC17 to FC22). They found that the impulse of the ankle plantarflexor moment was greatest during the high acceleration phase, and that the ankle and hip joints were two key sources of positive work across all three acceleration phases. Our results are in good agreement with these findings, but here we also reveal the important roles of the hamstrings and gluteus medius in accelerating the body forward during sprinting (Figure 5A). The contributions of soleus and gastrocnemius to the propulsive impulse were maximal during the high acceleration phase and they gradually reduced as forward acceleration decreased (or speed increased). In contrast, the contribution of hamstrings and gluteus medius remained relatively constant across all three acceleration phases. Such findings suggest that the ankle plantarflexors together with the hip extensors and abductors play a critical role in optimizing a sprinter's

performance when accelerating rapidly from a stationary position (Figure 6).

There are several limitations associated with our analyses. First, experimental data for the acceleration phase of sprinting were recorded in stages, with six different starting locations used for each participant. Ideally, data for all 19 foot contacts would have been recorded continuously within a single trial, but we did not have access to the instrumentation needed to calibrate a measurement space of this size. Second, data from five participants were used in the analysis presented here. Although a total of eight sub-elite sprinters participated in this study, data from all 19 foot contacts were recorded from only five participants. Data from the remaining three participants could not be analyzed over the entire acceleration phase because the foot contacted two force plates simultaneously at some foot falls. Third, a single representative trial from each participant was used to analyze each of the 19 foot contacts. A larger number of trials, while more desirable, would also have increased fatigue of our participants. Fourth, muscle forces were determined by solving an optimization problem that minimized the sum of muscle activations squared at each time instant during the stance phase of accelerated sprinting. This cost function has been used in musculoskeletal modeling studies to estimate lower-limb muscle forces during walking,²⁶ running³ and steady-speed sprinting.^{2,19} In addition, Lai et al.¹⁹ and Debaere et al.¹⁷ used CMC with a squared muscle activation minimization criterion to study lower-limb muscle function during accelerated sprinting. While a minimum-muscle-activation criterion may not be the most appropriate cost function for simulating explosive movements such as accelerated sprinting, our computed muscle activations were consistent with the sequence and timing of measured EMG signals (Figure S5), and the model-predicted muscle forces also accurately reproduced the required net joint moments generated at all foot contacts (Figure 2). Fifth, participant-specific models of our sprinters were created by scaling a generic model of a healthy adult to each participant's body anthropometry. To account for differences in lower-limb muscle strength between the generic model and sprinters, all muscles in the participant-specific models were assigned a two-fold increase in the nominal peak isometric force. Miller et al.³⁵ reported non-uniform differences in lower-limb muscle volumes between elite sprinters and untrained controls. In particular, muscle volumes measured for the hip extensors (gluteus maximus and the hamstrings) and knee extensors (vasti) were significantly larger for elite sprinters compared to untrained controls.³⁵ The volumes measured for the medial and lateral gastrocnemius were also larger for elite sprinters compared to untrained controls, but these differences were not significant. These results suggest that the more proximal hip and knee extensors are significantly stronger in elite sprinters than untrained controls, but the difference in ankle plantarflexor strength appears to be less. An unintended consequence of

uniformly increasing muscle strength (i.e., peak isometric muscle force) in the model is that the relative contributions of the lower-limb muscles to the GRF impulse may have been skewed. Specifically, it is likely that the strengths of the ankle plantarflexors were overestimated by doubling the values of peak isometric muscle force specified in the generic model. Thus, our estimates of the contributions of the ankle plantarflexors to the vertical and fore-aft GRF impulses may have been overestimated and those of the hip extensors (gluteus maximus and hamstrings) underestimated. Although our calculations of potential muscle contributions describe the functional roles of individual muscles independent of muscle strength (Figure 4), these results are influenced by differences in musculoskeletal geometry (i.e., moment arms) that may exist even after the generic model is scaled to each participant's body anthropometry. Future studies should attempt to incorporate muscle morphological data obtained from elite sprinters in participant-specific models to more accurately simulate the biomechanics of maximum-effort sprinting. Finally, modelling the foot as a single rigid segment may have affected our estimates of the forces developed by the ankle plantarflexors (soleus and gastrocnemius). A portion of the load attributed to the plantarflexors in a one-segment model of the foot would likely be attributed to the intrinsic and extrinsic muscles of the foot in a two-segment model that includes the metatarsophalangeal joint.³⁷ We do not expect a more detailed model of the foot to alter the role of the ankle plantarflexors found here for accelerated sprinting, however the percentage contributions of the soleus and gastrocnemius to the propulsive and support impulses relative to other muscles will likely differ. While a two-segment model would provide a more accurate anatomical representation of the foot, tracking the motions of these separate segments is particularly challenging when participants are sprinting close to their top speed.

This study combined musculoskeletal modeling and gait data to better understand how individual lower-limb muscles support and accelerate the body forward during maximum acceleration sprinting. We found that soleus contributed 44% of the muscle-induced upward impulse required to support the body against gravity whereas gastrocnemius generated 37% of the muscle-induced propulsive impulse needed to increase forward momentum at each foot contact. The hamstrings contributed considerably to sprint performance (15% of the muscle-induced propulsive impulse) by accelerating the body forward throughout the stance phase at all foot contacts. Gluteus maximus and hamstrings extended the hip and decelerated the swinging leg in preparation for foot contact at the next step.

5 | PERSPECTIVE

Previous studies have analyzed the function of the individual lower-limb muscles at various steady-state running speeds,

including sprinting.^{2,3} Similar analyses have not been undertaken for the acceleration phase of maximum-effort sprinting beyond the first two steps. This is an important knowledge gap as top sprinters in a 100 m race attain their maximum speeds after a 30 to 50 m acceleration phase.³⁸ We found that the ankle plantarflexors (soleus and gastrocnemius) and hip extensors (hamstrings and gluteals) propel the body forward from a stationary position. Our findings will be of interest to coaches striving to optimize sprint performance in elite athletes. Given the high mechanical demands placed on the calf and hamstring muscles during maximum acceleration sprinting, performing this explosive task repetitively in training may deliver a potent functional strengthening stimulus for these muscles, which may be useful for injury prevention practices in sports that involve repetitive short-burst sprints.

ACKNOWLEDGEMENTS

This study was supported in part by an Australian Research Council Linkage Project Grant LP110100262. We thank Drs Hossein Jahanabadi and Nuray Korkmaz for their input on preliminary analyses. We also thank the staff of the Biomechanics Laboratory at the Australian Institute of Sport for use of their experimental facilities in this study.

CONFLICT OF INTEREST

The authors have no conflicts of interest to declare.

DATA AVAILABILITY STATEMENT

The data that support the findings of this study are available from the corresponding author upon reasonable request.

REFERENCES

- Krzysztof M, Mero A. A kinematics analysis of three best 100 m performances ever. *J Hum Kinet*. 2013;36(1):149-160.
- Dorn TW, Schache AG, Pandy MG. Muscular strategy shift in human running: dependence of running speed on hip and ankle muscle performance. *J Exp Biol*. 2012;215(11):1944-1956.
- Hamner SR, Delp SL. Muscle contributions to fore-aft and vertical body mass center accelerations over a range of running speeds. *J Biomech*. 2013;46(4):780-787.
- Mann R, Sprague P. A kinetic analysis of the ground leg during sprint running. *Res Q Exerc Sport*. 1980;51(2):334-348.
- Bezodis IN, Kerwin DG, Salo AI. Lower-limb mechanics during the support phase of maximum-velocity sprint running. *Med Sci Sports Exerc*. 2008;40(4):707-715.
- Schache AG, Blanch PD, Dorn TW, Brown NA, Rosemond D, Pandy MG. Effect of running speed on lower limb joint kinetics. *Med Sci Sports Exerc*. 2011;43(7):1260-1271.
- Miller RH, Umberger BR, Hamill J, Caldwell GE. Evaluation of the minimum energy hypothesis and other potential optimality criteria for human running. *Proc Biol Sci*. 2012;279(1733):1498-1505.
- Carrier DR, Heglund NC, Earls KD. Variable gearing during locomotion in the human musculoskeletal system. *Science*. 1994;265(5172):651-653.
- Hunter JP, Marshall RN, McNair P. Relationships between ground reaction force impulse and kinematics of sprint-running acceleration. *J Appl Biomech*. 2005;21(1):31-43.
- Kugler F, Janshen L. Body position determines propulsive forces in accelerated running. *J Biomech*. 2010;43(2):343-348.
- Rabita G, Dorel S, Slawinski J, et al. Sprint mechanics in world-class athletes: a new insight into the limits of human locomotion. *Scand J Med Sci Sports*. 2015;25(5):583-594.
- Nagahara R, Mizutani M, Matsuo A, Kanehisa H, Fukunaga T. Association of sprint performance with ground reaction forces during acceleration and maximal speed phases in a single sprint. *J Appl Biomech*. 2018;34(2):104-110.
- Schache AG, Lai AKM, Brown NAT, Crossley KM, Pandy MG. Lower-limb joint mechanics during maximum acceleration sprinting. *J Exp Biol*. 2019;222(Pt 22):jeb209460.
- Morin JB, Gimenez P, Edouard P, et al. Sprint acceleration mechanics: the major role of hamstrings in horizontal force production. *Front Physiol*. 2015;6(404):404.
- Bartlett JL, Sumner B, Ellis RG, Kram R. Activity and functions of the human gluteal muscles in walking, running, sprinting, and climbing. *Am J Phys Anthropol*. 2014;153(1):124-131.
- Lieberman DE, Raichlen DA, Pontzer H, Bramble DM, Cutright-Smith E. The human gluteus maximus and its role in running. *J Exp Biol*. 2006;209(Pt 11):2143-2155.
- Debaere S, Delecluse C, Aerenhouts D, Hagman F, Jonkers I. Control of propulsion and body lift during the first two stances of sprint running: a simulation study. *J Sports Sci*. 2015;33(19):2016-2024.
- Hermens HJ, Freriks B, Disselhorst-Klug C, Rau G. Development of recommendations for SEMG sensors and sensor placement procedures. *J Electromyogr Kinesiol*. 2000;10(5):361-374.
- Lai A, Schache AG, Brown NA, Pandy MG. Human ankle plantar flexor muscle-tendon mechanics and energetics during maximum acceleration sprinting. *J R Soc Interface*. 2016;13(121):20160391.
- Lai AKM, Arnold AS, Wakeling JM. Why are antagonist muscles co-activated in my simulation? A musculoskeletal model for analysing human locomotor tasks. *Ann Biomed Eng*. 2017;45(12):2762-2774.
- Delp SL, Anderson FC, Arnold AS, et al. OpenSim: open-source software to create and analyze dynamic Simulations of movement. *IEEE Trans Biomed Eng*. 2007;54(11):1940-1950.
- Kristianslund E, Krosshaug T, van den Bogert AJ. Effect of low pass filtering on joint moments from inverse dynamics: implications for injury prevention. *J Biomech*. 2012;45(4):666-671.
- Thelen DG, Anderson FC. Using computed muscle control to generate forward dynamic simulations of human walking from experimental data. *J Biomech*. 2006;39(6):1107-1115.
- Lin Y-C, Kim HJ, Pandy MG. A computationally efficient method for assessing muscle function during human locomotion. *Int J Numer Meth Biomed Engng*. 2011;27(3):436-449.
- Liu MQ, Anderson FC, Pandy MG, Delp SL. Muscles that support the body also modulate forward progression during walking. *J Biomech*. 2006;39(14):2623-2630.
- Pandy MG, Lin Y-C, Kim HJ. Muscle coordination of mediolateral balance in normal walking. *J Biomech*. 2010;43(11):2055-2064.
- Schache AG, Lin Y-C, Crossley KM, Pandy MG. Is running better than walking for reducing hip joint loads? *Med Sci Sports Exerc*. 2018;50(11):2301-2310.
- Steele KM, DeMers MS, Schwartz MH, Delp SL. Compressive tibiofemoral force during crouch gait. *Gait Posture*. 2012;35(4):556-560.

29. Karabulut D, Dogru SC, Lin Y-C, Pandy MG, Herzog W, Arslan YZ. Direct validation of model-predicted muscle forces in the cat hindlimb during locomotion. *J Biomech Eng*. 2020;142(5):051014.
30. Martin JA, Brandon SCE, Keuler EM, et al. Gauging force by tapping tendons. *Nat Commun*. 2018;9:1592.
31. Nagahara R, Naito H, Morin JB, Zushi K. Association of acceleration with spatiotemporal variables in maximal sprinting. *Int J Sports Med*. 2014;35(9):755-761.
32. Matsuo A, Mizutani M, Nagahara R, Fukunaga T, Kanehisa H. External mechanical work done during the acceleration stage of maximal sprint running and its association with running performance. *J Exp Biol*. 2019;222(Pt 5):jeb189258.
33. Morin JB, Slawinski J, Dorel S, et al. Acceleration capability in elite sprinters and ground impulse: push more, brake less? *J Biomech*. 2015;48(12):3149-3154.
34. Marzke MW, Longhill JM, Rasmussen SA. Gluteus maximus muscle function and the origin of hominid bipedality. *Am J Phys Anthropol*. 1988;77(4):519-528.
35. Miller R, Balshaw TG, Massey GJ, et al. The muscle morphology of elite sprint running. *Med Sci Sports Exerc*. 2021;53(4):804-815.
36. Jacobs R, Bobbert MF, van Ingen Schenau GJ. Mechanical output from individual muscles during explosive leg extensions: the role of biarticular muscles. *J Biomech*. 1996;29(4):513-523.
37. Zelik KE, Honert EC. Ankle and foot power in gait analysis: implications for science, technology and clinical assessment. *J Biomech*. 2018;75:1-12.
38. Mero A, Komi PV, Gregor RJ. Biomechanics of sprint running. A review. *Sports Med*. 1992;13(6):376-392.

SUPPORTING INFORMATION

Additional supporting information may be found online in the Supporting Information section.

How to cite this article: Pandy MG, Lai AKM, Schache AG, Lin Y-C. How muscles maximize performance in accelerated sprinting. *Scand J Med Sci Sports*. 2021;31:1882–1896. <https://doi.org/10.1111/sms.14021>